BMB Reports - Manuscript Submission

Manuscript Draft

Manuscript Number: BMB-18-064

Title: Anti-inflammatory effects of a novel compound, MPQP, through the inhibition of IRAK1 signaling pathways in LPS-stimulated RAW 264.7 macrophages

Article Type: Article

Keywords: Inflammation; MPQP; IL-1 receptor-associated kinase 1; cyclooxygenase 2; inflammatory cytokine

Corresponding Author: Sayeon Cho

Authors: Ba Reum Kim[1], Young-Chang Cho[2], Sayeon Cho[1,*]

Institution: [1]College of Pharmacy, Chung-Ang University,
[2]College of Pharmacy, Chonnam National University,

Manuscript Type: Article

Title: Anti-inflammatory effects of a novel compound, MPQP, through the inhibition of IRAK1 signaling pathways in LPS-stimulated RAW 264.7 macrophages

Author's name: Ba Reum Kim[1], Young-Chang Cho[2], and Sayeon Cho[1,*]

Affiliation: [1]College of Pharmacy, Chung-Ang University, Seoul 06974, Republic of Korea

[2]College of Pharmacy, Chonnam National University, Gwang-ju, 61186, Republic of Korea;

Running Title: Anti-inflammatory role of MPQP

Keywords: Inflammation, 1-[(2R,4S)-2-methyl-4-(phenylamino)-1,2,3,4-tetrahydroquinolin-1-yl]prop-2-en-1-one, IL-1 receptor-associated kinase 1, cyclooxygenase 2, inflammatory cytokine

***Corresponding Author:** Tel.: +82 2 820 5595, Fax: +82 2 816 7338, E-mail address: sycho@cau.ac.kr

ABSTRACT

Small-molecule inhibitors are widely used to treat a variety of inflammatory diseases. In this study, we found a novel anti-inflammatory compound, 1-[(2R,4S)-2-methyl-4-(phenylamino)-1,2,3,4-tetrahydroquinolin-1-yl]prop-2-en-1-one (MPQP). It showed strong anti-inflammatory effects in lipopolysaccharide (LPS)-stimulated RAW 264.7 macrophages. These effects were exerted through the inhibition of the production of NO and pro-inflammatory cytokines, such as interleukin (IL)-6, IL-1β, and tumor necrosis factor-α (TNF-α). Furthermore, MPQP decreased the expression levels of inducible NO synthase (iNOS) and cyclooxygenase 2 (COX-2). Additionally, it mediated the inhibition of the phosphorylation of p38, c-Jun N-terminal kinase (JNK), the inhibitor of κBα (IκBα), and their upstream kinases, IκB kinase (IKK) α/β, mitogen-activated protein kinase kinase (MKK) 3/6, and MKK4. Furthermore, the expression of IL-1 receptor-associated kinase 1 (IRAK1) that regulates NF-κB, p38, and the JNK signaling pathways, was also increased by MPQP. These results indicate that MPQP regulates the IRAK1-mediated inflammatory signaling pathways by targeting IRAK1 or its upstream factors.

INTRODUCTION

Inflammation plays a key role in eliminating the initial causes of tissue injury and harmful stimuli such as pathogens and damaged cells (1). Inflammation is initiated by several immune cells including macrophages, dendritic cells, and monocytes upon stimulation (2). These immune cells produce various inflammatory mediators including nitric oxide (NO), prostaglandin E_2 (PGE_2), and pro-inflammatory cytokines such as interleukin (IL)-6, IL-1β, and tumor necrosis factor-α (TNF-α). These mediators induce the classical symptoms of inflammation including pain, heat, and swelling (3). However, the excessive production of pro-inflammatory mediators results in cellular damage and causes various inflammatory diseases (4). Therefore, the suppression of pro-inflammatory mediators is an attractive therapeutic strategy for the treatment of various inflammatory diseases.

The pro-inflammatory mediators are regulated by several signaling pathways including the nuclear factor-κB (NF-κB) and the mitogen-activated protein kinases (MAPKs). Upon stimulation of the macrophages with lipopolysaccharide (LPS), NF-κB and MAPKs are activated by cascades including IL-1 receptor-associated protein kinases (IRAKs) and the transforming growth factor-β-activated kinase 1 (TAK1). In the LPS-induced inflammation, the toll-like receptor 4 (TLR4) recognizes LPS and causes the activation of downstream signaling factors including myeloid differentiation factor 88 (MyD88), IRAKs, and TAK1 (5). When LPS binds to TLR4, the latter recruits MyD88, IRAKs, and other adaptor molecules. Association with MyD88 leads to IRAK4 activation and the phosphorylation of IRAK1 by IRAK4 (6). Phosphorylated IRAK1 activates the TRAF6/TAK1 complex to activate the downstream protein kinases, which are inhibitors of κB kinase (IKK) and MAPKs (6, 7).

IRAK1 is then polyubiquitinated by the IRAK1-activated E3 ligase and degraded by proteasomes (8). Activated IKK and MAPKs upregulate various transcription factors including NF-κB and activator protein-1 (AP-1) that induce the expression of pro-inflammatory mediators.

Small-molecule inhibitors are used for the treatment of various diseases and as tools to study the mechanisms of various cellular processes through the regulation of specific targets (9). In addition, small-molecule inhibitors are more stable than larger molecules (such as monoclonal antibodies), are generally cell-permeable, and can be easily used to compare, *in vivo*, the activity of analogs with diverse *in vitro* activities (9, 10). Previous studies have revealed a variety of small-molecule inhibitors with anti-inflammatory properties (11, 12). In this study, we screened 4,160 chemicals using NO production assays and found a novel small-molecule inhibitor, 1-[(2R,4S)-2-methyl-4-(phenylamino)-1,2,3,4-tetrahydroquinolin-1-yl] prop-2-en-1-one, named MPQP (Fig. 1A). Its inhibitory effects and the possible mechanism of action were studied by assessing the inflammatory signal transduction in LPS-stimulated RAW 264.7 macrophages.

RESULTS AND DISCUSSION

MPQP inhibits NO production in RAW 264.7 macrophages

Changes in the LPS-induced expression of pro-inflammatory mediators at the mRNA and protein levels in RAW 264.7 macrophages were measured by dose-dependent analysis to establish appropriate experimental conditions for evaluation of the anti-inflammatory effect of the chemicals. The mRNA expression levels of pro-inflammatory mediators (*iNOS*, *COX-2*, *IL-6*, *IL-1β*, and *TNF-α*) were increased until LPS concentration reached 100 ng/ml, but they were not increased any more at higher concentrations (Supplementary Fig. 1A). However, protein expression levels of iNOS and COX-2 were increased until LPS concentration reached 1 μg/ml of LPS (Supplementary Fig. 1B). We, therefore, used 100 ng/ml LPS for detection of mRNA and 1 μg/ml LPS for detection of protein in subsequent experiments, respectively.

NO assay was used as the primary screening tool to discover novel inflammatory inhibitors since NO analysis is less expensive, easier, and faster than other methods. We screened 4,160 chemicals for inhibitory effects on LPS-induced NO production and cell viability using RAW 264.7 macrophages at a constant concentration of 10 μM. Among candidates that inhibited NO production and showed no effect on cell viability, MPQP exhibited strong inhibitory effect on NO production compared to the LPS-control group.

To further evaluate the inhibitory effects of MPQP in LPS-induced inflammation, RAW 264.7 macrophages were pre-treated with MPQP at the indicated concentrations. MPQP was observed to significantly reduce the LPS-induced NO production in a dose-dependent manner without causing cytotoxicity (Fig. 1B and C). Since NO is synthesized by

inducible NO synthase (iNOS) on LPS stimulation, we tested the effects of MPQP on *iNOS* mRNA expression. The mRNA expression levels of *iNOS* were measured using RT-qPCR and semiquantitative PCR, as previously described (13). The decrease in NO levels was due to the reduced mRNA expression of the *iNOS* gene as shown by RT-qPCR (Fig. 1D). Semiquantitative PCR data verified the inhibitory effects of MPQP on the LPS-induced *iNOS* mRNA expression (Fig. 1E). Reduced *iNOS* mRNA expression resulted in the decreased expression of iNOS at the protein level (Fig. 1F). These results suggest that MPQP suppresses the LPS-induced NO production in RAW 264.7 macrophages through the regulation of the *iNOS* gene expression.

MPQP reduces cyclooxygenase 2 (COX-2) expression in RAW 264.7 macrophages

Next, we measured the COX-2 expression levels in the MPQP-treated macrophages since COX-2 is a general inflammatory mediator. As an enzyme that synthesizes PGE_2, it leads to inflammatory responses such as redness, swelling, and pain (14). MPQP significantly decreased the *COX-2* gene expression as determined by RT-qPCR (Fig. 2A). Additionally, semiquantitative RT-PCR showed that MPQP reduced the LPS-induced *COX-2* mRNA expression levels (Fig. 2B). Due to the decreased mRNA expression of *COX-2*, MPQP treatment led to a decreased expression of COX-2 at the protein level (Fig. 2C). These results indicate that MPQP may play a role in the regulation of PGE_2 production by inhibiting the *COX-2* gene expression at the transcription level.

MPQP suppresses the production of pro-inflammatory cytokines in RAW 264.7 macrophages

The production of pro-inflammatory cytokines is an important process that accompanies

LPS-stimulation in macrophages (15). Hence, we measured the effects of MPQP on the production of these pro-inflammatory cytokines, including IL-1β, IL-6, and TNF-α, in LPS-stimulated RAW 264.7 macrophages. As shown in Figure 2D, MPQP treatment showed a dose-dependent decrease in TNF-α production. In addition, MPQP strongly inhibited the production of IL-6 (Fig. 2D). To verify whether MPQP regulates the LPS-induced production of the cytokines at the mRNA expression level, we tested its effects on the gene expression by RT-qPCR and semiquantitative RT-PCR. The mRNA expression of IL-1β, IL-6, and TNF-α in the RAW 264.7 macrophages was significantly reduced by MPQP treatment (Fig. 2E and F). These results suggest that MPQP modulates the transcription factors that are involved in the production of the pro-inflammatory cytokines in the LPS-stimulated RAW 264.7 macrophages.

Interestingly, MPQP showed differential inhibitory effects on the LPS-induced production of pro-inflammatory mediators (Fig. 1 and 2). In particular, the inhibitory effects on NO, COX-2, and IL-6 production was observed to be higher than those of the other mediators including IL-1β and TNF-α (Fig. 1 and 2). Since these effects were regulated at the mRNA expression level by several signaling pathways, we estimated that MPQP might differentially regulate each LPS-stimulated signaling pathway. There are several signaling pathways such as NF-κB and MAPKs, including extracellular signal-regulated kinase (ERK), p38, and c-Jun N-terminal kinases (JNK), that are activated by LPS stimulation. When these signaling pathways are suppressed by each specific inhibitor, different inhibitory effects on the production of the pro-inflammatory mediators were observed. For example, SP600125, a specific JNK inhibitor, significantly inhibits the LPS-induced production of NO, IL-6, IL-1β,

and TNF-α, but not COX-2. On the other hand, specific ERK inhibitors (U0126 and PD98059) strongly decrease the production of COX-2 but have little effect on the production of IL-6 and TNF-α (16-18). Similar to these studies, our results suggest that MPQP probably has anti-inflammatory effects through the selective inhibition of specific signaling pathways.

MPQP inhibits IκBα, p38, and JNK phosphorylation in LPS-stimulated RAW 264.7 macrophages

In LPS-stimulated inflammation, the two major transcription factors, NF-κB and AP-1, are activated by LPS-induced upstream kinases such as IκBα and MAPKs. LPS-induced NF-κB activation occurs via the phosphorylation of IκBα at Ser-32/36 followed by degradation, which results in the release and nuclear translocation of NF-κB (19). AP-1 is a dimeric transcription factor composed of Jun, Fos, or ATF (activating transcription factor), and is upregulated through phosphorylation by MAPKs (20). MAPKs are activated through phosphorylation in the activation loops by MAPK kinases (21). To test the effects of MPQP on the LPS-induced activation of the NF-κB and MAPK signaling pathways, we analyzed the phosphorylation levels of IκBα and MAPKs in the LPS-stimulated RAW 264.7 macrophages upon treatment with MPQP. The phosphorylation levels of IκBα were attenuated and the IκBα expression was increased upon MPQP treatment in a dose-dependent manner (Fig. 3A). Furthermore, the phospho (p)-p38 and p-JNK levels were decreased after MPQP treatment without changing the total p38 and JNK levels, whereas p-ERK levels were observed to be unchanged (Fig. 3B). These results suggest that MPQP selectively inhibits pro-inflammatory responses through the inhibition of NF-κB, p38, and JNK signaling pathways.

MPQP suppresses the activation of upstream kinases including IKKα/β, MAPK kinase (MKK) 3/6, and IRAK1 in LPS-stimulated RAW 264.7 macrophages

Since MPQP inhibited the phosphorylation of IκBα, p38, and JNK, these molecular targets of MPQP were further investigated by examining their upstream kinases. Upon LPS stimulation, the phosphorylation of IκBα, p38, and JNK requires the activation of upstream kinases including IKKα/β, MKK3/6, and MKK4, respectively. Therefore, we examined whether MPQP was able to inhibit the phosphorylation of these upstream kinases. Treatment of RAW 264.7 macrophages with MPQP decreased p-IKKα/β, p-MKK3/6, and p-MKK4 in a dose-dependent manner. These results suggest that MPQP regulates a further upstream regulator that commonly modulates these signals (Fig. 3C and D). Since the activation of IKKα/β, MKK3/6, and MKK4 occurs after LPS-induced activation and degradation of IRAK1 (6, 7), we examined whether MPQP regulates the expression level of IRAK1. In RAW 264.7 macrophages, the expression level of IRAK1 was measured after LPS treatment. As a result, the expression level of IRAK1 decreased after 5 min of LPS treatment (Supplementary Fig. 1). When RAW 264.7 macrophages were pre-treated with MPQP prior to the LPS stimulation, MPQP suppressed the degradation of IRAK1 (Fig. 3D). These data suggest that MPQP might regulate the expression of pro-inflammatory mediators by acting on far upstream signaling proteins such as IRAK1 or its upstream factors (Fig. 4).

When we examined the effects of the IRAK specific inhibitor (*N*-[1-[2-(4-Morpholinyl)ethyl]-1*H*-benzimidazol-2-yl]-3-nitrobenzamide) on LPS-stimulated inflammation in RAW 264.7 macrophages, the IRAK inhibitor showed anti-inflammatory effects similar to MPQP in LPS-stimulated RAW 264.7 macrophages (Supplementary Fig. 3A

and B). It reduced the phosphorylation of IκBα, p38, JNK, IKKα/β, MKK4, and MKK3/6 as well as degradation of IRAK1. In addition, the IRAK inhibitor significantly inhibited NO production without cytotoxicity (Supplementary Fig. 4A and B). Furthermore, the IRAK inhibitor showed stronger inhibitory effects on the LPS-induced expression of IL-6, IL-1β, and iNOS than COX-2 and TNF-α (Supplementary Fig. 4C and D), suggesting similar effects as MPQP.

In this study, we investigated the anti-inflammatory effects of MPQP, which is one of the many quinoline derivatives that possess diverse pharmacological properties including anti-microbial, analgesic, and anti-carcinogenic effects (22-24). There are several studies reporting the anti-inflammatory effects of quinoline derivatives (25). In general, quinoline derivatives modulate the inflammatory responses associated with TNF-α, thereby suppressing chronic inflammatory diseases such as psoriasis, Crohn's disease, and rheumatoid arthritis (26, 27). However, the anti-inflammatory effects of MPQP are exhibited through the inhibition of LPS-induced IRAK1 activation. Reduction of inflammation by the inhibition of IRAK1 signaling may contribute to the regulation of chronic as well as acute inflammatory responses (28, 29).

MPQP inhibited IL-6 production more strongly than other inflammatory cytokines. IL-6 is involved in the development of various inflammatory diseases, including rheumatoid arthritis, cancer, and osteoporosis (30-32). So far, various peptide drugs including tocilizumab, which blocks the effect of IL-6 by inhibiting its binding to IL-6 receptor for the treatment of RA and systemic juvenile idiopathic arthritis, have been available (33, 34). However, the limitation of administration site based on the dosage form of peptide drugs led to the trial for

the discovery of IL-6-inhibiting chemicals. Since MPQP significantly inhibited LPS-induced IL-6 production at low dose (1 μM) with little regulatory effects on the other inflammatory mediators in RAW 264.7 cells, MPQP has the potential as a therapeutic candidate for the treatment of IL-6-dominant inflammatory diseases.

Based on previous studies and our results, it is expected that MPQP could provide a new perspective on the regulation of LPS-stimulated inflammation by quinoline derivatives through the inhibition of LPS-induced IRAK1 activation. In conclusion, the results of this study suggest that MPQP might be useful in the treatment of various inflammatory diseases through the inhibition of IRAK1-mediated inflammatory signals.

MATERIALS AND METHODS

See Supplementary information.

ACKNOWLEDGMENTS

We thank the cooperation of Korea Chemical Bank to use chemical library for screening (http://www.chembank.or.kr). This work was supported by the National Research Foundation of Korea (NRF) grants funded by the Korean government (Ministry of Science and ICT) (NRF-2018R1A2B6005084 and 2015R1A5A1008958).

CONFLICTS OF INTEREST

The authors have no conflicting financial interests.

REFERENCES

1. Kim, E., Yang, W. S., Kim, J. H., et al. (2014) Lancemaside A from Codonopsis lanceolata modulates the inflammatory responses mediated by monocytes and macrophages. Mediators Inflamm. 2014, 405158-405158.
2. Nowarski, R., Gagliani, N., Huber, S. and Flavell, R. A. (2013) Innate immune cells in inflammation and cancer. Cancer Immunol Res 1, 77-84.
3. Wu, L.-c., Fan, N.-c., Lin, M.-h., et al. (2008) Anti-inflammatory effect of spilanthol from Spilanthes acmella on murine macrophage by down-regulating LPS-induced inflammatory mediators. J. Agric. Food Chem. 56, 2341-2349.
4. Libby, P. (2007) Inflammatory mechanisms: the molecular basis of inflammation and disease. Nutr. Rev. 65, S140-S146.
5. Barton, G. M. and Medzhitov, R. (2003) Toll-like receptor signaling pathways. Sci 300, 1524-1525.
6. Ordureau, A., Smith, H., Windheim, M., et al. (2008) The IRAK-catalysed activation of the E3 ligase function of Pellino isoforms induces the Lys63-linked polyubiquitination of IRAK1. Biochem. J. 409, 43-52.
7. Avila, M. and Gonzalez-Espinosa, C. (2011) Signaling through Toll-like receptor 4 and mast cell-dependent innate immunity responses. IUBMB Life 63, 873-880.
8. Jiang, Z., Ninomiya-Tsuji, J., Qian, Y., Matsumoto, K. and Li, X. (2002) Interleukin-1 (IL-1) receptor-associated kinase-dependent IL-1-induced signaling complexes phosphorylate TAK1 and TAB2 at the plasma membrane and activate TAK1 in the cytosol. Mol. Cell. Biol. 22, 7158-7167.

9. Schreiber, S. L. (1998) Chemical genetics resulting from a passion for synthetic organic chemistry. Biorg. Med. Chem. 6**,** 1127-1152.

10. Thompson, L. A. and Ellman, J. A. (1996) Synthesis and applications of small molecule libraries. Chem. Rev. 96**,** 555-600.

11. Chen, W., Wang, J., Luo, Y., et al. (2016) Ginsenoside Rb1 and compound K improve insulin signaling and inhibit ER stress-associated NLRP3 inflammasome activation in adipose tissue. J Ginseng Res 40**,** 351-358.

12. Cha, B.-J., Park, J.-H., Shrestha, S., et al. (2015) Glycosyl glycerides from hydroponic Panax ginseng inhibited NO production in lipopolysaccharide-stimulated RAW264. 7 cells. J Ginseng Res 39**,** 162-168.

13. Cho, Y.-C., Kim, Y. R., Kim, B. R. and Cho, S. (2016) Thunbergia alata inhibits inflammatory responses through the inactivation of ERK and STAT3 in macrophages. Int. J. Mol. Med. 38**,** 1596-1604.

14. Funk, C. D. (2001) Prostaglandins and leukotrienes: advances in eicosanoid biology. Sci 294**,** 1871-1875.

15. Feghali, C. A. and Wright, T. M. (1997) Cytokines in acute and chronic inflammation. Front. Biosci. 2**,** d12-d26.

16. Ma, P., Liu, H.-T., Wei, P., et al. (2011) Chitosan oligosaccharides inhibit LPS-induced over-expression of IL-6 and TNF-α in RAW264. 7 macrophage cells through blockade of mitogen-activated protein kinase (MAPK) and PI3K/Akt signaling pathways. Carbohydr. Polym. 84**,** 1391-1398.

17. Kwak, H. J., Song, J. S., Heo, J. Y., Yang, S. D., Nam, J.-Y. and Cheon, H. G. (2005) Roflumilast inhibits lipopolysaccharide-induced inflammatory mediators via

suppression of nuclear factor-κB, p38 mitogen-activated protein kinase, and c-Jun NH2-terminal kinase activation. J. Pharmacol. Exp. Ther. 315, 1188-1195.

18. Lee, J., Tae, N., Lee, J. J., Kim, T. and Lee, J.-H. (2010) Eupatolide inhibits lipopolysaccharide-induced COX-2 and iNOS expression in RAW264. 7 cells by inducing proteasomal degradation of TRAF6. Eur. J. Pharmacol. 636, 173-180.

19. Finco, T. S., Beg, A. A. and Baldwin, A. S. (1994) Inducible phosphorylation of I kappa B alpha is not sufficient for its dissociation from NF-kappa B and is inhibited by protease inhibitors. Proc. Natl. Acad. Sci. U. S. A. 91, 11884-11888.

20. Karin, M., Liu, Z.-g. and Zandi, E. (1997) AP-1 function and regulation. Curr. Opin. Cell Biol. 9, 240-246.

21. Plotnikov, A., Zehorai, E., Procaccia, S. and Seger, R. (2011) The MAPK cascades: signaling components, nuclear roles and mechanisms of nuclear translocation. BBA Molecular Cell Research 1813, 1619-1633.

22. Neu, H. C. (1992) Quinolone antimicrobial agents. Annu. Rev. Med. 43, 465-486.

23. Abadi, A. H., Hegazy, G. H. and El-Zaher, A. A. (2005) Synthesis of novel 4-substituted-7-trifluoromethylquinoline derivatives with nitric oxide releasing properties and their evaluation as analgesic and anti-inflammatory agents. Biorg. Med. Chem. 13, 5759-5765.

24. Solomon, V. R. and Lee, H. (2011) Quinoline as a privileged scaffold in cancer drug discovery. Curr. Med. Chem. 18, 1488-1508.

25. Kumar, S., Bawa, S. and Gupta, H. (2009) Biological activities of quinoline derivatives. Mini Rev. Med. Chem. 9, 1648-1654.

26. Dinarello, C. A. (2010) Anti-inflammatory agents: present and future. Cell 140, 935-

950.

27. Palladino, M. A., Bahjat, F. R., Theodorakis, E. A. and Moldawer, L. L. (2003) Anti-TNF-α therapies: the next generation. Nature Reviews Drug Discovery 2**,** 736-742.

28. Kim, S.-J., Cha, J.-Y., Kang, H. S., et al. (2016) Corosolic acid ameliorates acute inflammation through inhibition of IRAK-1 phosphorylation in macrophages. BMB Reports 49**,** 276-281.

29. Li, M., Yu, D., Ni, B. and Hao, F. (2017) Interleukin-1 receptor associated kinase 1 is a potential therapeutic target of anti-inflammatory therapy for systemic lupus erythematosus. Mol. Immunol. 87**,** 94-101.

30. Nishimoto, N. (2006) Interleukin-6 in rheumatoid arthritis. Curr. Opin. Rheumatol. 18**,** 277-281.

31. Anestakis, D., Petanidis, S., Kalyvas, S., et al. (2015) Mechanisms and αpplications of ınterleukins in cancer immunotherapy. Int. J. Mol. Sci. 16**,** 1691-1710.

32. Scheidt-Nave, C., Bismar, H., Leidig-Bruckner, G., et al. (2001) Serum interleukin 6 is a major predictor of bone loss in women specific to the first decade past menopause. J. Clin. Endocrinol. Metab. 86**,** 2032-2042.

33. Smolen, J. S. and Maini, R. N. (2006) Interleukin-6: a new therapeutic target. Arthrit. Res. Ther. 8**,** S5.

34. Emery, P., Keystone, E., Tony, H., et al. (2008) IL-6 receptor inhibition with tocilizumab improves treatment outcomes in patients with rheumatoid arthritis refractory to anti-tumour necrosis factor biologicals: results from a 24-week multicentre randomised placebo-controlled trial. Ann. Rheum. Dis. 67**,** 1516-1523.

FIGURE LEGENDS

Figure 1. Chemical structure and inhibitory effects of MPQP on the NO production without cytotoxicity. (A) Chemical structure of MPQP. (B, C, D, E, and F) RAW 264.7 macrophages were incubated with MPQP (1, 2, 5, and 10 μM) for 2 h and then stimulated with LPS for the indicated time periods. (B) After LPS (1 μg/ml) stimulation for 24 h, cell viability was measured using EZ-Cytox solution. Cell viability values are shown as bar graphs compared to the LPS-treated group (100%). (C) After 24 h LPS (1 μg/ml) stimulation, the NO production levels were measured using Griess reagents and are shown as bar graphs according to the standard curve calculated on the basis of the nitrite standard solution. (D and E) After 3 h LPS (100 ng/ml) stimulation, total RNA was extracted and reverse transcribed to cDNA. (D) *iNOS* was amplified by qPCR and the expression levels of *iNOS* are shown as bar graphs compared to the LPS-treated group (100%). (E) *iNOS* was amplified by PCR and visualized using EtBr staining. The relative expression level of *iNOS* was normalized to *GAPDH* levels. Quantitative analyses of mRNA expression levels are shown as fold changes following normalization. (F) Total cell lysates were prepared after 24 h LPS (1 μg/ml) stimulation and analyzed by immunoblot analysis. The expression levels of iNOS were detected using specific antibodies. The relative expression levels of iNOS were normalized to α-tubulin levels. Quantitative analyses of the protein levels are shown as fold changes following normalization. The relative expression levels of iNOS are presented as a bar graph. All bar graphs are represented as the mean ± SEM and analyzed using one-way ANOVA for the significance between the three independent experiments. $^{\#}p<0.0001$ vs. LPS-untreated control groups. $^{a}p<0.01$ and $^{b}p<0.001$ vs. LPS-treated groups.

Figure 2. Inhibitory effects of MPQP on the expression levels of COX-2 and the production of pro-inflammatory cytokines. RAW 264.7 macrophages were incubated with MPQP (1, 2, 5, and 10 μM) for 2 h and stimulated with LPS for the indicated time periods. (A, B, E, and F) After 3 h LPS (100 ng/ml) stimulation, total RNA was extracted and reverse transcribed to cDNA. (A) *COX-2* was amplified by qPCR and the expression levels of *COX-2* are shown as bar graphs compared to the LPS-treated group (100%). (B) *COX-2* was amplified by PCR and visualized by EtBr staining. The relative expression level of *COX-2* was normalized to the *GAPDH* levels. Quantitative analyses of mRNA expression levels are shown as fold changes following normalization. (C) Total cell lysates were prepared after 24 h LPS (1 μg/ml) stimulation and analyzed by immunoblot analysis. The expression levels of COX-2 were detected using specific antibodies. The relative expression levels of COX-2 were normalized to α-tubulin levels. Quantitative analyses of protein levels are shown as fold changes after normalization. (D) After 24 h LPS (1 μg/ml) stimulation, ELISA was carried out to measure the levels of TNF-α and IL-6. The production of each cytokine was measured using a standard curve. (E) *IL-1β*, *IL-6*, and *TNF-α* were amplified by qPCR and their expression levels are shown as bar graphs compared to the LPS-treated group (100%). (F) *IL-1β*, *IL-6*, and *TNF-α* were amplified by PCR and visualized by EtBr staining. The relative expression levels of *IL-1β*, *IL-6*, and *TNF-α* were normalized to GAPDH levels. Quantitative analyses of the mRNA expression levels are shown as fold changes following normalization. All bar graphs are represented as the mean ± SEM and analyzed using one-way ANOVA from three independent experiments. $^{\#}p<0.0001$ vs. LPS-untreated control groups. $^{a}p<0.01$ and $^{b}p<0.001$ vs LPS-treated groups.

Figure 3. Inhibitory effects of MPQP on LPS-induced NF-κB and MAPK pathways. RAW 264.7 macrophages were pre-incubated with MPQP (1, 2, 5, and 10 μM) for 2 h and stimulated with LPS (1 μg/mL) for 5 min (for detection of IκBα, IKKα/β, and IRAK1) or 15 min (for detection MAPKs, MKK3/6, and MKK4). Total cell lysates were prepared and analyzed by immunoblot analysis. The expression levels of (A) p-IκBα, IκBα, (B) p-JNK, JNK, p-ERK, ERK, p-p38, p38, (C) p-MKK3/6, MKK3/6, p-MKK4, MKK4, (D) IRAK1, p-IKKα/β, and IKKα/β were detected using specific antibodies. The relative expression levels of p-IκBα, IκBα, and IRAK1 were normalized to the α-tubulin levels. The phosphorylation levels of MAPKs, MKK3/6, MKK4, and IKKα/β were normalized to the corresponding MAPKs, MKK3/6, MKK4, and IKKα/β levels. Quantitative analyses of phosphorylation and protein levels are shown as bar graphs after normalization. All bar graphs are represented as the mean ± SEM and analyzed using one-way ANOVA from three independent experiments. $^{\#}p<0.0001$ vs. LPS-untreated control groups. $^{a}p<0.01$ and $^{b}p<0.001$ vs LPS-treated groups.

Figure 4. **Schematic representation of the anti-inflammatory effects of MPQP on the LPS-induced inflammatory pathway.** MPQP inhibited LPS-induced activation of IRAK1 or its upstream factors and sequentially suppressed the activation of downstream kinases. As a result of IRAK1 inhibition, the expression of pro-inflammatory mediators was decreased.

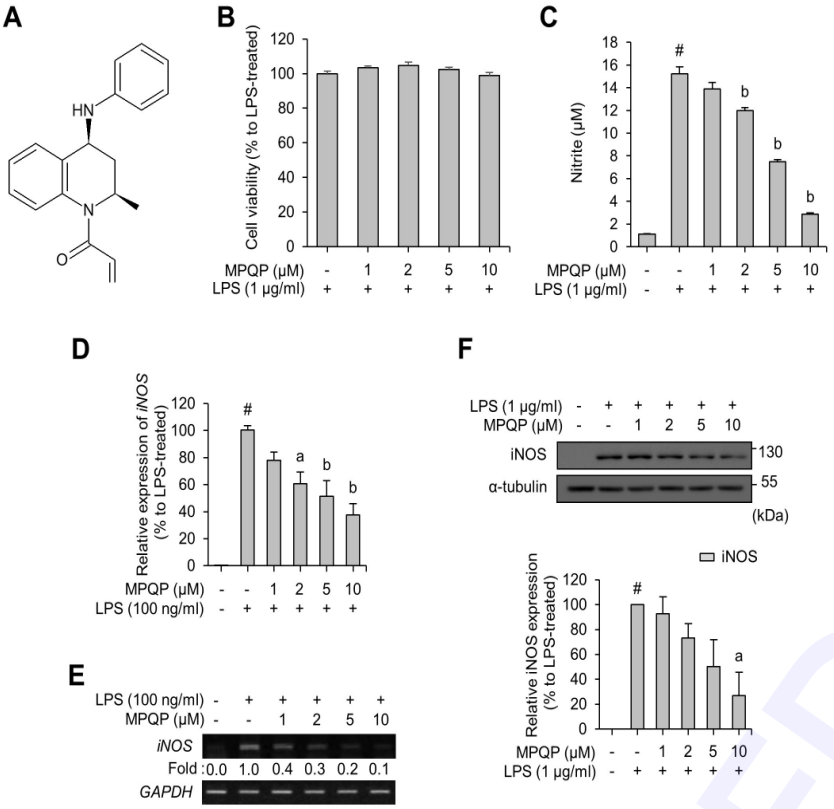

Figure 1

Fig. 1.

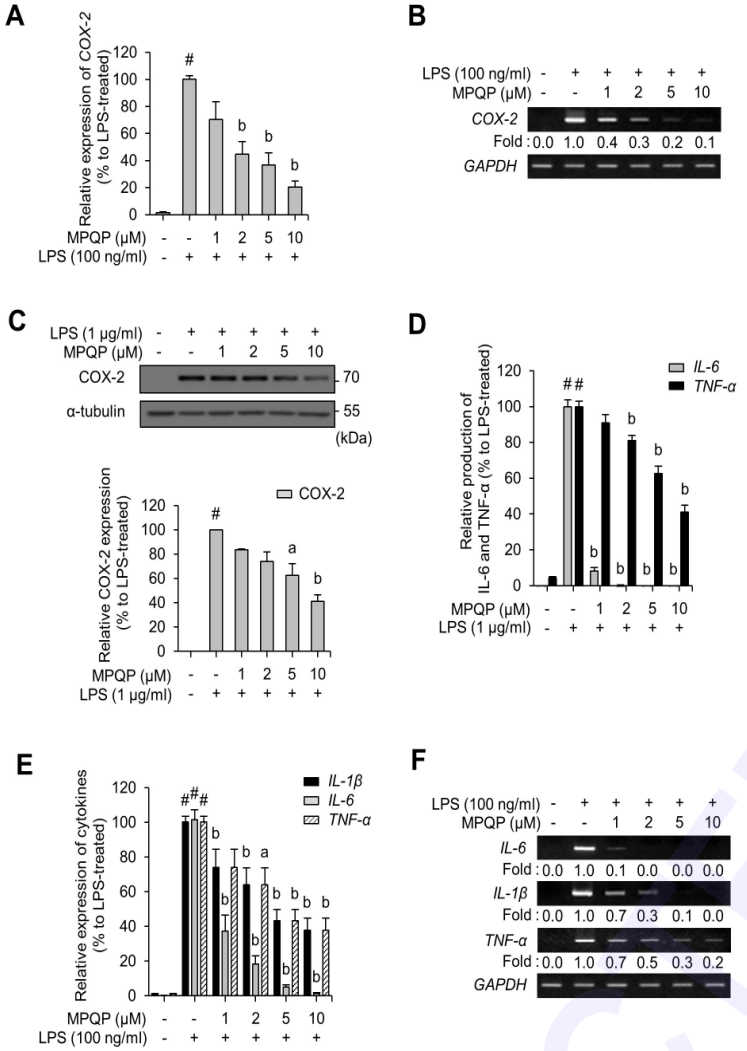

Figure 2

Fig. 2.

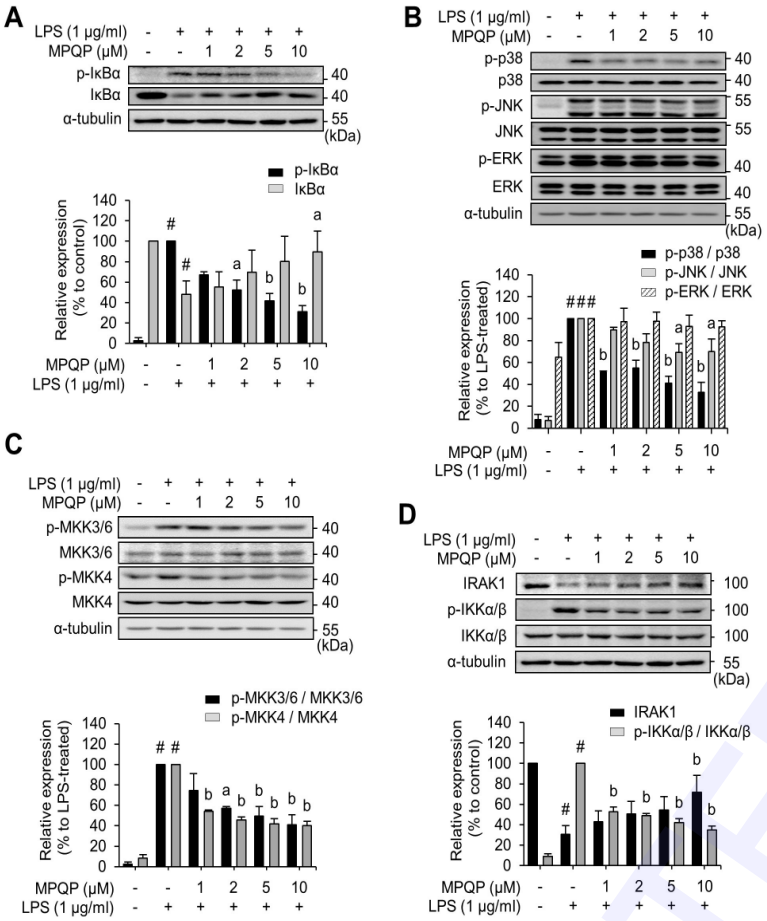

Figure 3

Fig. 3.

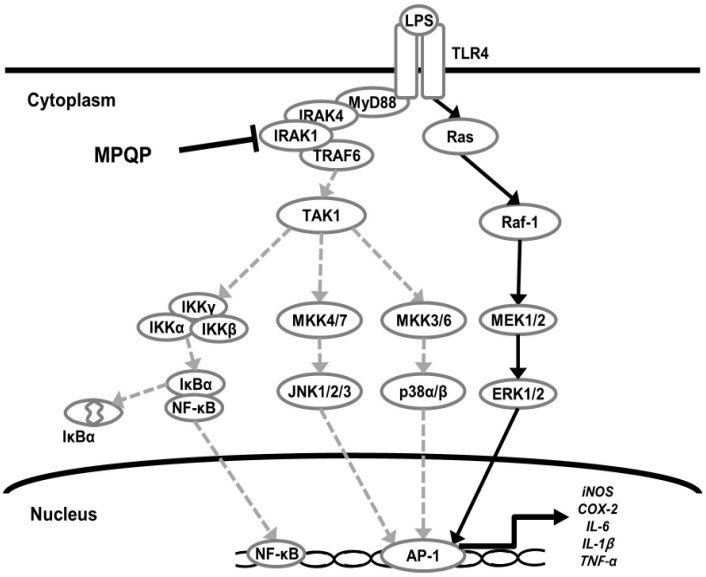

Figure 4

Fig. 4.

Manuscript Type: Article

Title: Anti-inflammatory effects of a novel compound, MPQP, through the inhibition of IRAK1 signaling pathways in LPS-stimulated RAW 264.7 macrophages

Author's name: Ba Reum Kim[1], Young-Chang Cho[2], and Sayeon Cho[1,*]

Affiliation: [1]College of Pharmacy, Chung-Ang University, Seoul 06974, Republic of Korea

[2]College of Pharmacy, Chonnam National University, Gwang-ju, 61186, Republic of Korea;

Running Title: Anti-inflammatory role of MPQP

Keywords: Inflammation, 1-[(2R,4S)-2-methyl-4-(phenylamino)-1,2,3,4-tetrahydroquinolin-1-yl]prop-2-en-1-one, IL-1 receptor-associated kinase 1

Corresponding Author's Information: Tel.: +82 2 820 5595, Fax: +82 2 816 7338, E-mail address: sycho@cau.ac.kr

Supplementary information:

Supplementary file 1: Supplementary information.

Supplementary file 2: Supplementary figure 1 – 4

1. MATERIALS AND METHODS

Reagents and antibodies

A chemical library containing 4,160 compounds was provided by Korea Chemical Bank (Daejeon, Korea). 1-[(2R,4S)-2-methyl-4-(phenylamino)-1,2,3,4-tetrahydroquinolin-1-yl]prop-2-en-1-one (MPQP; STOCK1S-54010, C19H20N2O, M.W.: 292.382, and purity: 95%) was purchased from InterBioScreen Ltd. (Moscow, Russia). Rabbit anti-p-IκBα (Ser-32/36; cat. no. sc-101713), anti-IκBα (cat. no. sc-371), anti-IKKα/β (cat. no. 7607), mouse anti-p38 (cat. no. sc-7972), anti-JNK (cat. no. sc-7345), anti-MKK3/6 (cat. no. 133230), anti-IRAK1 (cat. no. sc-5288), and anti-α-tubulin (cat. no. sc-8035) antibodies were purchased from Santa Cruz Biotechnology, Inc. (Dallas, TX, USA). Rabbit anti-p-p38 (Thr-180/Tyr-182; cat. no. 9211), anti-p-JNK (Thr-183/Tyr-185; cat. no. 9251), anti-p-ERK (Thr-202/Tyr-204; cat. no. 9101), anti-ERK (cat. no. 9102), anti-p-MKK3/6 (Ser-189/207; cat. no. 9231), anti-p-MKK4 (Thr-261; cat. no. 9151), anti-MKK4 (cat. no. 9152), anti-p-IKKα/β (Ser-176/180; cat. no. 2697), anti-iNOS (cat. no. 2982), and anti-COX-2 (cat. no. 4842) antibodies were purchased from Cell Signaling Technology, Inc. (Danvers, MA, USA). Goat anti-rabbit IgG (cat. no. LF-SA8002) and anti-mouse IgG (cat. no. LF-SA8001) were purchased from Abfrontier (Seoul, Korea). Goat anti-mouse IgM (cat. no. ADI-SAB-110-J) was purchased from Enzo Life Sciences, Inc. (Farmingdale, New York, USA). DMSO was purchased from

Sigma-Aldrich; Merck KGaA (Darmstadt, Germany). EZ-Cytox solution was purchased from Daeil Lab Service Co., Ltd. (Seoul, Korea). Ready-SET-Go! ELISA kits for the detection of IL-6 (cat. no. 88-7064) and TNF-α (cat. no. 88-7324) were from eBioscience (San Diego, CA, USA). Accuzol reagent was from Bioneer Corporation (Daejeon, Korea) and TOPscript cDNA synthesis kit was from Enzynomics Co., Ltd. (Daejeon, Korea). The iTaq Universal SYBR Green Supermix was obtained from Bio-Rad Laboratories, Inc. (Hercules, CA, USA). Ethidium bromide (EtBr) was purchased from Invitrogen (Carlsbad, CA, USA). IRAK specific inhibitor (*N*-[1-[2-(4-Morpholinyl)ethyl]-1*H*-benzimidazol-2-yl]-3-nitrobenzamide, CAS 509093-47-4) was purchased from Tocris Bioscience (Ellisville, MO, USA) (1).

Cell culture

RAW 264.7 macrophages (mouse monocytic cell line; ATCC, Manassas, VA, USA) were maintained in Dulbecco's Modified Eagle's medium (Hyclone, Logan, UT, USA) containing 10% fetal bovine serum (Hyclone), 50 U/ml penicillin and 50 µg/ml streptomycin (Gibco; Thermo Fisher Scientific, Inc., Waltham, MA, USA) at 37˚C in humidified air containing 5% CO_2.

Chemical library screening

Cells were seeded in 96-well plates ($4.0x10^4$ cells/well) and incubated at 37˚C overnight. Cells were pre-treated with 4,160 compounds at a constant concentration of 10 µM for 2 h and stimulated with LPS treatment (1 µg/ml). After LPS stimulation for 24 h, the inhibitory effect of each compound on LPS-induced inflammation was evaluated by analyzing LPS-induced NO production using Griess reagent. Cell viability assay was used to test the

cytotoxicity of each compound. All experiments were independently repeated three times with triplicate samples.

Measurement of Cell Viability

RAW 264.7 macrophages were pre-treated with MPQP (1, 2, 5, and 10 μM) for 2 h and then incubated for 24 h at 37˚C in the absence or presence of LPS (1 μg/ml). Following incubation, EZ-Cytox solution (1/20 dilution of culture medium) was added to each well and incubated for 1 h. Supernatants were transferred to 96-well plates and the absorbance was measured at 450 nm using Synergy H1 Microplate reader (BioTek Instruments, Inc., Winnoski, VT, USA).

Measurement of NO Production

NO was measured as its stable oxidative metabolite, nitrite (NOx), as previously described (2). Cells were seeded in 96-well plate ($4.0x10^4$ cells/well) and incubated at 37˚C overnight. Cells were pre-treated with various concentrations of MPQP (1, 2, 5, and 10 μM) for 2 h prior to LPS treatment. Following stimulation with LPS (1 μg/ml) for 24 h, the supernatants (100 μl) were transferred to a new 96-well plate and 100 μl Griess reagent (1% sulfanilamide, 0.1% N-1-naphthylenediamine dihydrochloride and 2.5% phosphoric acid) was added to each well. $NaNO_2$ solution (2.5, 5, 10, 25, 50, and 100 μM) was used to generate standard curve for calculating the quantity of NO in supernatants. The absorbance was measured at 540 nm using Synergy H1 Microplate reader (BioTek Instruments, Winooski, VT, USA).

Enzyme-linked immunosorbent assay (ELISA)

The cells were seeded in 96-well plates ($4.0x10^4$ cells/well) and incubated at 37˚C overnight. They were pre-treated with various concentrations of MPQP (1, 2, 5, and 10 μM) for 2 h prior to the LPS treatment as previously described (3). Following stimulation with LPS (1 μg/ml) for 24 h, the supernatants were collected and diluted according to the predetermined dilution rates for each of the pro-inflammatory cytokines. The production of pro-inflammatory cytokines, including IL-6 and TNF-α, was measured using Ready-SET-Go! ELISA kits for each of the cytokines according to manufacturer's protocol. Briefly, the 96-well plates were coated with coating solution overnight at 4˚C and washed thrice with 1X phosphate-buffered saline/0.05% Tween 20 (PBST). Subsequently, they were treated with 1X Assay Diluent for 1 h at room temperature (RT). After the wells were emptied, diluted supernatants and standard solutions were added to each well. After 2 h at RT, the plates were washed thrice with 1X PBST and the detection antibody solution diluted in 1X Assay Diluent was added. The plates were washed following a 1 h treatment, horseradish peroxidase-streptavidin solution was added for 30 min. The plates were subsequently washed 5 times. A solution of 3,3',5,5'-tetramethylbenzidine (TMB) was added to the plates which were then incubated for 10 min in the dark. To stop the reaction, 1 N H_3PO_4 was added to the plate and the absorbance of each well was measured using the Synergy H1 Microplate reader at 450 nm.

Semiquantitative RT-PCR and RT-qPCR

The mRNA expression levels of pro-inflammatory mediators were measured using semiquantitative RT-PCR and RT-qPCR as previously described (3). Cells were seeded in 12-well plate ($8.0x10^5$ cells/well) and incubated at 37˚C overnight. Cells were pre-treated with

various concentrations of MPQP (1, 2, 5, and 10 μM) for 2 h prior to LPS treatment. After LPS (100 ng/ml) stimulation for 3 h, total RNA was prepared from cells and reverse-transcribed into cDNA using a TOP-script™ cDNA synthesis kit (Enzynomics, Daejeon, Korea). For supplementary figure 1, RAW 264.7 macrophages were stimulated with LPS to identify the changes of mRNA expression levels of pro-inflammatory mediators in dose-dependent manner (50, 100, 500, and 1000 ng/ml for 3 h).

The semiquantitative PCR was run for 17-25 cycles at 94˚C for 30 s, 60˚C for 30 s, and 72˚C for 30 s using a thermal cycler (Bioer Technology Co., Hangzhou, China). Following amplification, 10 μl of the PCR products were separated in 1.5% (w/v) agarose gels and visualized by EtBr staining. PCR primers used in these experiments were listed in the previous report (4).

RT-qPCR amplification of the cDNA was performed using iTaq Universal SYBR Green Supermix, according to the manufacturer′s protocol. The PCR was run for 40 cycles of denaturation at 94˚C for 5 s and annealing/extension at 60˚C for 30 s using a CFX Connect real-time thermal cycler (Bio-Rad Laboratories, Inc.). Based on the $2^{-\Delta\Delta Cq}$ method (5), the results were normalized to multireference genes, β-actin and GAPDH. The results were expressed as the ratio of gene expression to the LPS treated group (100%). PCR primers used in these experiments were listed in the previous report (4).

Immunoblot Analysis

RAW 264.7 macrophages pre-treated with MPQP were further stimulated with LPS (1 μg/ml) for the optimized time for the detection of target proteins (IκBα, IKKα/β, and IRAK1 for 5 min; MAPKs, MKK3/4, and MKK4 for 15 min; iNOS and COX-2 for 24 h). In

supplementary figures, RAW 264.7 macrophages were stimulated with LPS to identify the changes of protein expression levels of iNOS and COX-2 in dose-dependent manner (50, 100, 500, and 1000 ng/ml for 24 h).

Following stimulation for indicated times, cells were washed 3 times with ice-cold PBS. Lysis buffer, containing 0.5% IGEPAL, 0.5% Triton X-100, 150 mM NaCl, 20 mM Tris-HCl (pH 8.0), 1 mM EDTA, 1% glycerol, 1 mM phenylmethylsulfonyl fluoride (PMSF), 10 mM NaF, and 1 mM Na_3VO_4, was added to the washed wells and then collected in each microtube after 10 min. Following centrifugation at 15814 x *g* for 30 min at 4˚C, the supernatants were used for the experiments.

Protein concentrations were measured using the Bradford reagent (Bio-Rad Laboratories, Inc.). Aliquots of the samples were separated by 10% SDS-PAGE and transferred to nitrocellulose membranes with transfer buffer [192 mM glycine, 25 mM Tris-HCl (pH 8.8), and 20% methanol (v/v)]. Following blocking with 5% non-fat dried milk in 1X Tris-buffered saline with 0.05% Tween 20 (TBST), each membrane was incubated overnight at 4˚C with primary antibodies (1:1000 for all primary antibodies). Each membrane was incubated for an additional 1 h with secondary peroxidase-conjugated IgG (1:5,000) at RT. After washing 5 times with 1X TBST, the target proteins were detected using enhanced chemiluminescence (Thermo Fisher Scientific, Inc.). Protein levels were quantified by scanning the immunoblots and analyzing them with LabWorks software version 4.6 (UVP, LLC; Analytik Jena AG, Upland, CA, USA).

Statistical analysis

The bar data are represented as the mean ± standard error of the mean. Comparisons between multiple experimental groups were performed using one-way analysis of variance (ANOVA) followed by Dunnett's post-hoc test using GraphPad Prism (version 3.0; GraphPad Software, Inc., La Jolla, CA, USA) and $p<0.01$ was considered statistically significant. For the NO production, ELISA, and RT-qPCR analyses, the data from nine replicates were analyzed, including three independent experiments with three replicates each. For the immunoblotting analyses, the data from three independent experiments were analyzed.

2. SUPPLEMENTARY FIGURE LEGENDS

Supplementary Fig. 1. Dose-dependent expression levels of LPS-induced pro-inflammatory mediators. (A) RAW 264.7 macrophages were stimulated with LPS (50, 100, 500, and 1,000 ng/ml) for 3 h. Total RNA was extracted and reverse transcribed to cDNA. *iNOS*, *COX-2, IL-6, IL-1β,* and *TNF-α* were amplified by PCR and visualized by EtBr staining. (B) RAW 264.7 macrophages were stimulated with LPS (50, 100, 500, and 1,000 ng/ml) for 24 h. Total cell lysates were prepared and analyzed by immunoblot analysis. The expression levels of iNOS, COX-2, and α-tubulin were detected using specific antibodies.

Supplementary Fig. 2. Time-dependent expression levels of IRAK1 upon LPS stimulation. RAW 264.7 macrophages were stimulated with LPS (1 μg/ml) for 1, 3, 5, and 10 min. Total cell lysates were prepared and analyzed by immunoblot analysis. The expression level of IRAK1 and α-tubulin were detected using specific antibodies.

Supplementary Fig. 3. Inhibitory effects of the IRAK specific inhibitor on LPS-induced NF-κB and MAPK pathways. RAW 264.7 macrophages were pre-treated with the IRAK specific inhibitor (10 μM) for 2 h and stimulated with LPS (1 μg/ml) for 5 min (for detection of IRAK1, IKKα/β, and IκBα) or 15 min (for detection MKK3/6, MKK4, and MAPKs). Total cell lysates were prepared and analyzed by immunoblot analysis. The expression levels of (A) IRAK1, p-IKKα/β, IKKα/β, p-IκBα, IκBα, (B) p-MKK3/6, MKK3/6, p-MKK4, MKK4, p-JNK, JNK, p-p38, p38, p-ERK, ERK, and α-tubulin were detected using specific antibodies. The relative expression levels of p-IκBα, IκBα, and IRAK1 were normalized to the α-tubulin

levels. The phosphorylation levels of MAPKs, MKK3/6, MKK4, and IKKα/β were normalized to the corresponding MAPKs, MKK3/6, MKK4, and IKKα/β levels.

Supplementary Fig. 4. Inhibitory effects of the IRAK specific inhibitor on LPS-induced inflammation. (A, B, and D) RAW 264.7 macrophages were pre-treated with the IRAK specific inhibitor (10 μM) for 2 h and stimulated with LPS (1 μg/ml) for 24 h. (A) Cell viability was measured using EZ-Cytox solution. Cell viability values are shown as bar graphs compared to the LPS-treated group (100%). (B) The NO production levels were measured using Griess reagents and shown as bar graphs according to the standard curve calculated on the basis of the nitrite standard solution. (C) RAW 264.7 macrophages were pre-treated with the IRAK specific inhibitor (10 μM) for 2 h and stimulated with LPS (100 ng/ml) for 3 h. Total RNA was extracted and reverse transcribed to cDNA. *iNOS*, *COX-2, IL-6, IL-1β,* and *TNF-α* were amplified by PCR and visualized by EtBr staining. (D) Total cell lysates were prepared and analyzed by immunoblot analysis. The expression levels of iNOS, COX-2, and α-tubulin were detected using specific antibodies. All bar data graphs are represented as the mean ± SEM and analyzed using one-way ANOVA for the significance between the three independent experiments. $^{\#}p<0.0001$ vs. LPS-untreated control groups. $^{a}p<0.01$ and $^{b}p<0.001$ vs LPS-treated groups.

REFERENCES

1. Powers, J. P., Li, S., Jaen, J. C., et al. (2006) Discovery and initial SAR of inhibitors of interleukin-1 receptor-associated kinase-4. Bioorg. Med. Chem. Lett. 16, 2842-2845.
2. Lee, K. J., Kim, Y. K., Krupa, M., et al. (2016) Crotamine stimulates phagocytic activity by inducing nitric oxide and TNF-α via p38 and NFκ-B signaling in RAW 264.7 macrophages. BMB Rep 49, 185.
3. Cho, Y.-C., Kim, Y. R., Kim, B. R. and Cho, S. (2016) Thunbergia alata inhibits inflammatory responses through the inactivation of ERK and STAT3 in macrophages. Int. J. Mol. Med. 38, 1596-1604.
4. Cho, Y.-C., Ju, A., Kim, B. R. and Cho, S. (2015) Anti-inflammatory effects of Crataeva nurvala Buch. Ham. are mediated via inactivation of ERK but not NF-κB. J. Ethnopharmacology 162, 140-147.
5. Livak, K. J. and Schmittgen, T. D. (2001) Analysis of relative gene expression data using real-time quantitative PCR and the 2− ΔΔCT method. Methods 25, 402-408.

Supplementary Figure 1

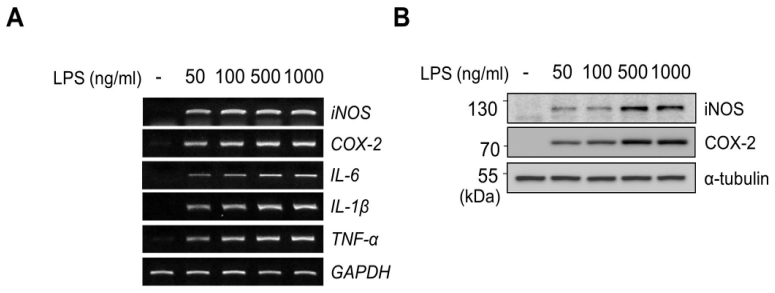

Sup. 2.

Supplementary Figure 2

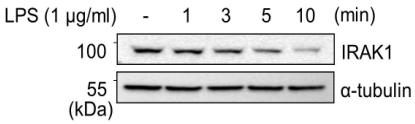

Sup. 3.

Supplementary Figure 3

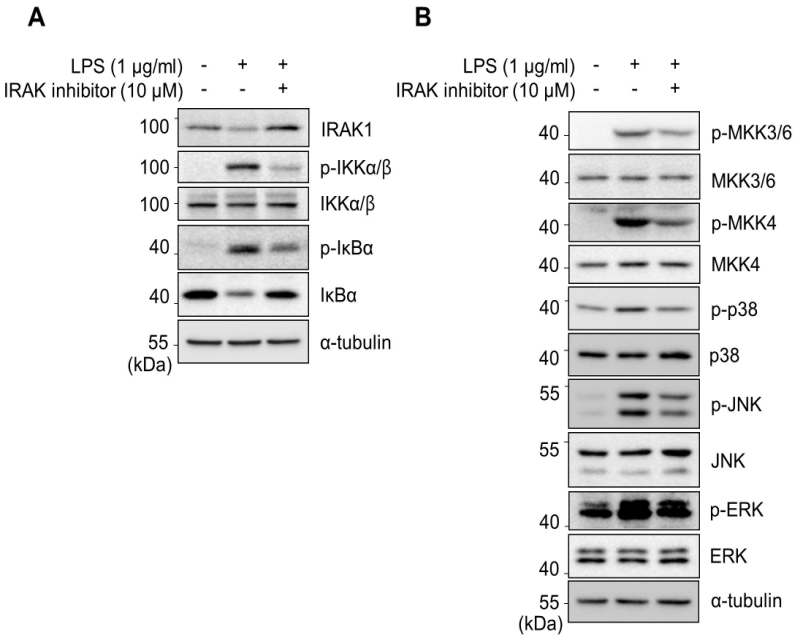

Sup. 4.

Supplementary Figure 4

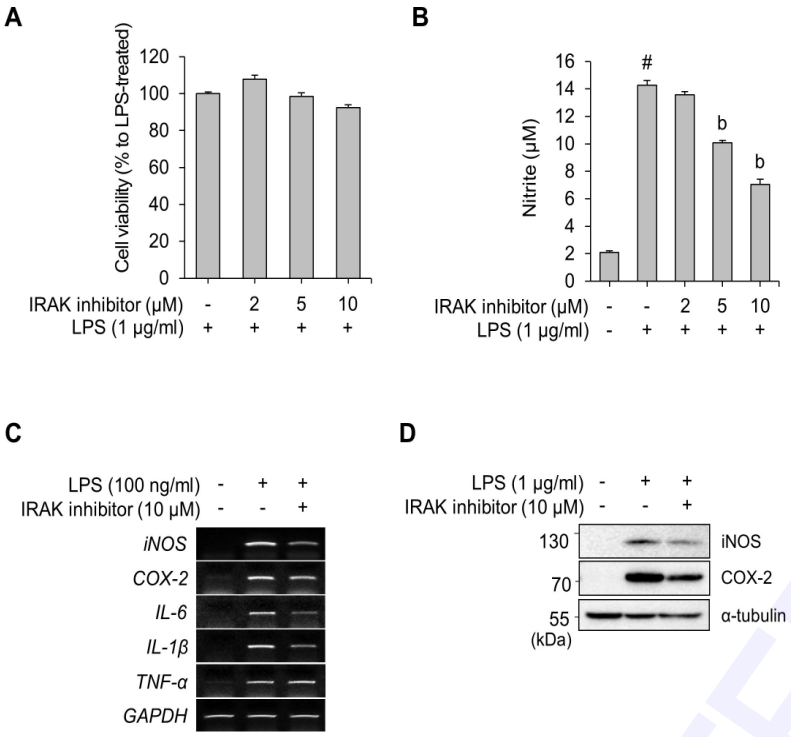

Sup. 5.